Building and Environment 118 (2017) 101–112

Contents lists available at ScienceDirect

Building and Environment

journal homepage: www.elsevier.com/locate/buildenv

Using multi-robot active olfaction method to locate time-varying contaminant source in indoor environment

Yicun Chen, Hao Cai**, Zhilong Chen*, Qilin Feng

State Key Laboratory of Explosion & Impact and Disaster Prevention & Mitigation, PLA University of Science and Technology, Nanjing, 210007, PR China

ARTICLE INFO

Article history:
Received 30 November 2016
Received in revised form
17 March 2017
Accepted 18 March 2017
Available online 23 March 2017

Keywords:
Active olfaction
Time-varying contaminant source
Multi-robot

ABSTRACT

Prevention of indoor contaminant source leak disasters is becoming an urgent issue in the indoor environment and public safety fields. Quickly locating such a source is a prerequisite for effective implementation of source control, and a key basis for further guidance on evacuation and emergency rescue. Indoor contaminant sources have many forms because of source characteristic variation. The current research focuses on continuous release from a source with constant intensity and instantaneous release from a source with impulse intensity. There are few studies of sources with varying release intensity. The main goal of the present research study was to develop a source localization method for a time-varying source. A computational fluid dynamics model of leakage for an indoor time-varying contaminant source is established, together with a search strategy using multi-robot active olfaction. Based on the time-varying leakage source localization method, the robots are used to verify method effectiveness through indoor two-dimensional ventilation room simulation experiments. The influence of factors such as intensity change, position and obstacles on the localization is analyzed, which provides a foundation for further study of contaminant source identification in an unsteady flow field.

1. Introduction

Personnel poisoning, fire, explosion and other disasters caused by leakage of indoor hazardous gas have occurred repeatedly in recent years. From 2010 to 2012, seven U.S. states including Louisiana, New York and North Carolina had 1369 oil leakage accidents, causing 36 fatalities and 512 injuries [1]. On August 12, 2015, an accidental explosion of hazardous chemicals in the Tianjin Binhai New Area of China sounded the alarm for prevention and control of leakage disasters involving indoor hazardous gas. Rapid localization of leakage sources is key to preventing and alleviating such disasters, by taking effective measures during emergencies with leakage of indoor hazardous gas [2].

Research into localization of indoor leakage sources is mainly concerned with two types of leakage sources: (1) A continuous release source with constant release rate and (2) instantaneous release source with impulse [3,4]. In an actual situation, there is one type of common leakage source, namely, a source with release intensity continuously varying with time [5]. With leakage of a pipeline orifice with an automatic turn-off device as an example, the entire leakage process can be deemed gas leakage in a rigid container of fixed volume, and the leakage rate continuously decreases with time. Theoretically, constant and impulse sources can also be considered an exception to a time-varying source. Hence, it is of realistic importance and theoretical value to research the localization of a time-varying source. However, there has been little research into such localization in the indoor environment at present.

Current localization methods of indoor leakage sources can be roughly divided into two types: fixed-sensor network and robot active olfactory. For the former method, one or more sensors are arranged in space and the location of the leakage source is inferred through the gas concentration detected by the sensor. The method mainly has two modes. One is such that numerous simulation computations are conducted in advance and stored in a database, and then a rapid gas diffusion model is used along with an efficient search algorithm. After leakage of the contaminant source, an approximate value is sought for each sensor concentration reading to obtain source characteristics, using for example a Bayesian probability method in combination with a multi-zone model [6,7], artificial neural network method [8,9] or optimization methods

* Corresponding author.
** Corresponding author.
E-mail addresses: caihaohvac@gmail.com (H. Cai), chen-zl@vip.163.com (Z. Chen).

http://dx.doi.org/10.1016/j.buildenv.2017.03.030
0360-1323/

Nomenclature

b_1	learning factor from itself
b_2	learning factor from entire swarm robots
c_i	fitness of i th robot
c_p	threshold value of plume finding
f_t	mass flux
F	boundary of control volume
k_1	leakage parameter depends on leakage characteristics and the surrounding environment
k_2	a constant depends on the ratio of specific heats of the gas at constant pressure and constant volume
l	side length of the regular octagon
n	total number of robots
P_i	location of i th robot
P_{pi}	location of i th robot when its maximum fitness value achieved
P_g	location of the robot when its fitness value achieved to maximum among entire swarm
Q	leakage rate of a contaminant source
R	particle swarm with robots
r_1,r_2	random numbers between 0 and 1
t	time
Δt	interval time of each iteration
$T_{\max}$	time threshold
V_i	velocity of i th robot
v	airflow velocity
w	inertia weight
W	control volume of a point source

Subscript

i	index of robot

with a limited number of simulations [10,11]. The other mode is such that the location of the contaminant source is determined by solving the control equation of gas diffusion via inverse analysis, with the sensor concentration as the initial condition. Common methods include quasi-reversibility [12], pseudo-reversibility [13], regularization [2], and probability-based inverse [14] methods.

The above works were largely based on a constant or transient source. Zhang et al. [15] used two sensors to first establish a release curve of the leakage source and then infer the location of that source according to Bayesian method, with identification of the source when its leakage intensity is continuously constant or varies in the form of a sine wave. Wang et al. [16] investigated the localization of a pollution source based on a fixed sensor with minimum dispersion and maximum correlation coefficient methods. However, the aforementioned works require certain preconditions, such as location, flow field of all possible leakage sources, variation curve of intensity of the leakage source and sensor, and other information. In addition, for localization of a time-varying source with decaying release intensity, there are no reports at present.

The robot active olfactory method is similar to the behavior of animals. For example, dogs, moths, lobsters and other animals usually identify and locate food sources, spy on natural enemies, mark routes, and seek spouses with initiative smell. An active olfactory source localization method based on the bionics principle "initiatively" searches for and determines the location of a leakage source with a searching algorithm using a mobile robot with sensor system, without the need for solving complicated gas diffusion equation [17–19]. Since the 1990s, Russel et al. [20] and Harvey et al. [21] have used smell and wind-direction sensors to research smell tracking and verify the validity of localization methods.

Active olfactory methods can be divided by quantity into multi-robot [22–24] and single-robot [21,25–27]. Relative to the single-robot method, the multi-robot active olfactory method can simplify a mobile robot, adapting better to a complicated flow field environment, and improve search efficiency and the success rate [28,29]. Hence, we used the multi-robot method to locate the leakage source.

For a time-varying contaminant source with decaying release intensity, localization of the robot active olfactory method is used for exploratory research. By using a diverging plume search strategy, particle swarm optimization (PSO) plume-tracking strategy, and source identification method of flux divergence, the validity of the robot active olfactory method in identification of a time-varying source is verified. To further reveal the influence of a time-varying contaminant source on active olfactory localization based on the multi-robot approach, we established environments with a barrier and other factors for a contaminant source with different release intensities and locations in a case analysis.

2. Active olfactory method based on multi-robot approach

2.1. Overview of active olfactory method

The trajectory of gas dispersion in a flow field is normally a plume [30]. Using this plume, active olfactory methods typically find the location of a leakage source in three stages: plume finding, plume traversal, and source declaration [31,32]. Among these, the most critical stage is plume traversal, which has attracted much attention in recent years.

Plume finding is a process in which robots search unknown areas and contact leakage gas using a certain plume-finding strategy. The strategy is normally developed using a bionics principle, which has major effects on the plume-finding efficiency. Common strategies include the passive monitoring method [20], spiral surge algorithm [33], zigzag traversal method [34], and levy-taxis algorithm [35].

Plume traversal refers to the process in which a robot approaches a leakage source using collected information such as gas concentration, wind velocity, and wind direction. According to the robots used, the plume traversal strategies can be roughly divided into two categories, single-robot and multi-robot. Single-robot strategies mainly include chemotaxis [36], anemotaxis [37], infotaxis [19,38], and vision and olfaction complex algorithms [26,39]. Multi-robot strategies can not only follow the principle of single-robot strategies, but can also leverage cooperation between multiple robots to cover a larger space and improve the efficiency and success rate of source tracking [28,29]. Common multi-robot strategies include the divergence of gradient-based algorithms [40], PSO method [41], and multi-agent search strategies [42].

Source declaration is the final process, which confirms whether the source location found is correct. There have been few research works reporting on source declaration, and major challenges remain to confirm a source in real-world environments [43]. Typical source declaration methods are the source identification zones [34,44], machine learning [32], divergence of mass flux [40], and particle filtering [41] methods.

2.2. Method to localize leakage source using PSO algorithm

The PSO algorithm has good performance in finding global extremum with high speed of convergence. But this algorithm is easy to be trapped into local minima [41]. To overcome this weakness, the PSO algorithm combined with divergence of mass flux method, which can help robots to avoid local minima and improve search efficiency. Furthermore, our method uses the divergence search strategy in the plume-finding stage, PSO algorithm in the plume traversal stage, and divergence of mass flux method in the leakage source declaration stage.

According to the divergence search strategy, the robots diverge from the same location at a constant speed. To cover as much area as possible, each robot moves in a straight line, and their trajectories uniformly divide the plane at sensor height into several identical angles.

The PSO algorithm is a novel optimization method based on swarm intelligence. This algorithm has been widely used in the fields of system design, target optimization, biological engineering, and disease treatment, owing to its powerful ability of global optimization [45]. The algorithm normally treats each individual as a particle without mass or size, and uses the value of fitness to evaluate whether a particle is at a proper location. To solve optimization questions in a complex environment, a particle swarm normally adjusts the movement of each particle via collaboration and information-sharing between particles [41].

In this paper, we treat each robot as a particle and a group of robots as a particle swarm. The i th robot is denoted R_i, and the particle swarm with n robots is denoted $R = (R_1, R_2, \cdots, R_i, \cdots, R_n)$. At moment$t$, the location, velocity, and fitness of R_i are denoted $P_i(t) = (x_i(t), y_i(t), z_i(t))^T$, $V_i(t) = (v_{ix}(t), v_{iy}(t), v_{iz}(t))^T$, and $c_i(t)$, respectively. The value of fitness is represented by the gas concentration at the location of the robot. Once a robot finds the plume, the group of robots move to the leakage source using the PSO algorithm (Fig. 1).

We assume that the fitness of particle R_i achieves its maximum value $c_{i\max}(t)$ at location $P_{pi} = (x_{pi}, y_{pi})^T$ during the period 0 through t. With the movement of each particle, the fitness of the entire particle swarm updates constantly and achieves its maximum value $c_{\max}(t)$ at location $P_g = (x_g, y_g)^T$. From time $t - \Delta t$ to t, the velocity and location of R_i update as follows:

$$\begin{cases} V_i(t) = w \times V_i(t-\Delta t) + b_1 \times r_1 \times (P_{pi} - P_i(t)) + b_2 \times r_2 \times (P_g - P_i(t)) \\ \begin{cases} V_i(t) = V_{\max}, & if \quad V_i(t) > V_{\max} \\ V_i(t) = V_{\min}, & if \quad V_i(t) < V_{\min} \end{cases} \end{cases}, \tag{1}$$

$$P_i(t) = P_i(t-\Delta t) + V_i(t)\Delta t, \tag{2}$$

where w is inertia weight, which represents the degree of inertial motion of a moving robot; b_1 and b_2 are learning factors that reflect the lessons learned by a robot from its movement and that of the robot swarm, respectively; Randomness is introduced via two independent random numbers r_1 and r_2 (between 0 and 1). In each iteration, the value of r_1 and r_2 are updated to improve the ability of robots to explore more space. $V_{\max}$ and $V_{\min}$ are the maximum and minimum speeds of a robot, respectively; This study focuses on validating the feasibility of the proposed method. For simplicity, we set w to 1.0, and set b_1 and b_2 to 1.2, according to the previous experience [46]. w was set to 1.0, both b_1 and b_2 were set to 1.2; $V_{\max}$ and $V_{\min}$ were set to 0.6 m/s and 0.0 m/s, respectively.

We set a time threshold $T_{\max}$ to make an initial determination of the location of the leakage source during the plume traversal process. If the maximum fitness of R remains unchanged for a period no less than $T_{\max}$, we assume that the robot swarm nearing the leakage source. Using the time threshold may cause misjudgment when a robot swarm gets trapped in local optimum area where the gas concentration is higher than in other areas but is far from the leakage source. Therefore, we also use mass the flux divergence method to make a final determination.

When a gas is continuously released from a point source, the mass flux of the gas near that point should be greater than zero, which can be expressed as [40]:

$$\oint_W \nabla \cdot (cv) dW = \oint_F (cv) \cdot dF, \tag{3}$$

where W is a control volume and F is its boundary.

To calculate mass flux, we use four robots to move around the suspected leakage source at the same speed. The tracks of the robots form a regular octagon within a circle, as shown in Fig. 2.

The mass flux f_t of the leakage gas can be calculated approximately as

$$f_t = \oint_F (cv) \cdot dF \approx \sum_i^4 (c_i(t-\Delta t) \times v_i(t-\Delta t) + c_i(t) \times v_i(t)) \times l, \tag{4}$$

where $c_i(t)$ and $v_i(t)$ are the gas concentration and airflow velocity detected by robot R_i at time t, respectively; l is the side length of the regular octagon.

The mass flux f_t of the gas far away from a point source should be less than zero. Therefore, we set 0 as the threshold of f_t. In practice, considering the existence of detection errors, we should set a specific value greater than zero as the threshold of f_t by trail-and-error or other method to prevent the missing of global optimum. If the calculated f_t is greater than 0, then we assume that the

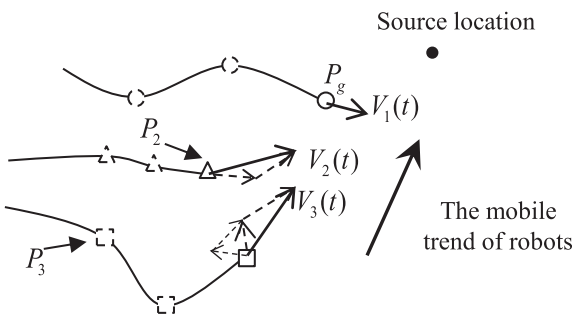

Fig. 1. Process of plume-tracking using PSO algorithm.

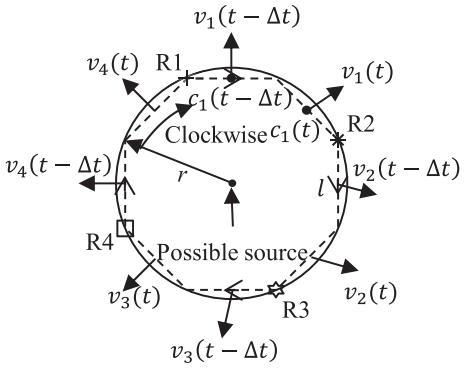

Fig. 2. Process to determine mass flux.

center of the regular octagon is near the leakage source. Otherwise, we assume that the robot swarm is trapped in a local optimum area.

In practice, each robot can be equipped with five ultrasonic sensors to detect an obstacle in front of the robot. We also designed an obstacle and robot avoidance algorithm. When a robot is approaching an obstacle (wall, desk, or other robot) at time t, the robot will calculate whether it will impact that obstacle at time $t+\Delta t$. If collision will occur, the robot will change direction and maintain the same speed of movement. Both intersection angles at time t and $t+\Delta t$ between the velocity of the robot and obstacle plane are of the same magnitude. If collision will occur between robots, the robot will vary its speed to avoid the other robot, under the premise of a fixed predicted location. A detailed description of the collision avoidance algorithm is given in Appendix A.

2.3. Procedure of source localization method

Our method is composed of three stages, as shown in Fig. 3. In the plume-finding stage, using the divergence search strategy, the robots diverge from the same location to cover as much area as possible. When a robot finds the plume, the entire robot swarm R switches to the plume traversal stage, in which the PSO algorithm is used to continuously update the maximum fitness of the robot swarm. If the maximum fitness of R remains unchanged for a period longer than $T_{\max}$, then the mass flux divergence method is used to make a further determination. Then, if the leakage source is confirmed, the source location is reported and the procedure is finished. Otherwise, each robot will remain at its location and initialize its fitness value to disregard the local optimum area, and then switch to the first stage to find the plume again.

3. Case setup

3.1. Basic assumptions and validation method

We used simulation experiments to verify the effectiveness of our method and illustrate its application. For simplicity, we made the following assumptions.

1. The robots are particles without any physical volume.

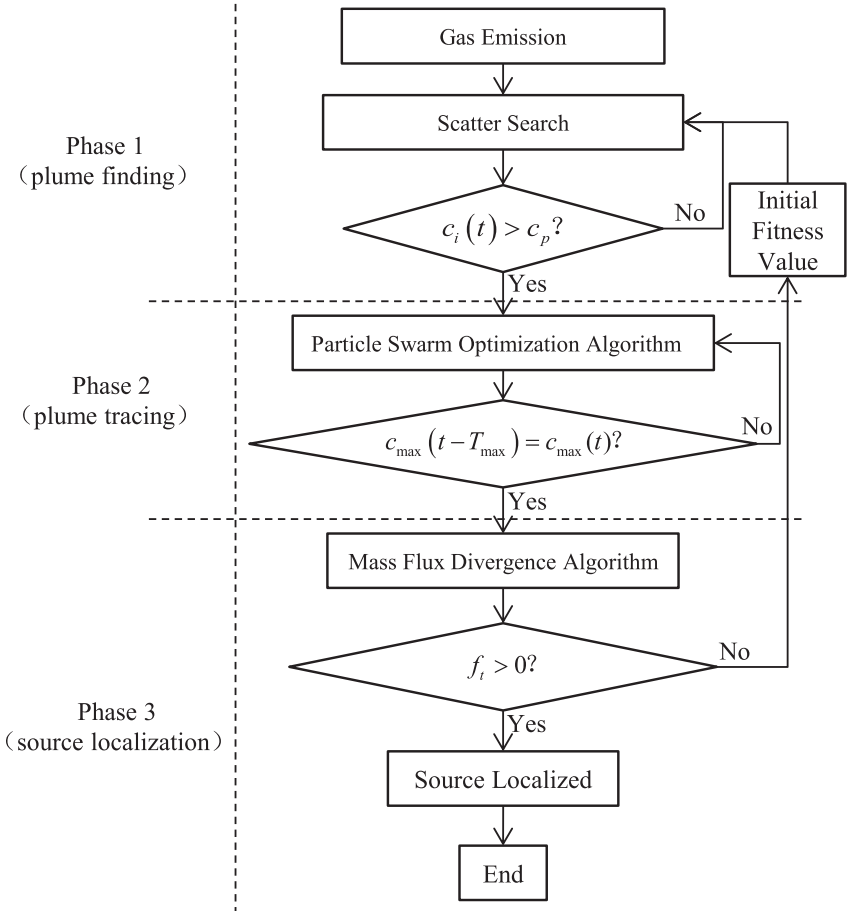

Fig. 3. Procedure of source identification method.

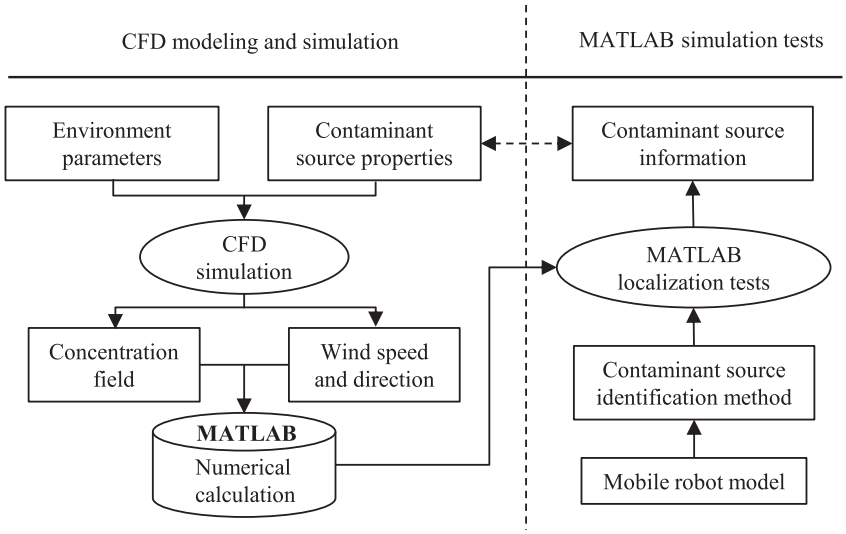

Fig. 4. Validation procedure of simulation experiment.

2. Robot movement does not affect the distribution of leakage gas.
3. The sensors can detect gas concentration, wind speed, and wind direction without any time delay.
4. The robots can communicate with each other to share data such as gas concentration, wind speed, and wind direction.

The procedure of the simulation experiment is shown in Fig. 4. First, with inputs of environmental parameters and source characteristics, we used commercial computational fluid dynamics (CFD) software FLUENT to obtain the steady airflow field and unsteady concentration field. Second, with the latter field, we conducted simulation experiments in MATLAB to test the effectiveness of the method.

3.2. Description of cases

We focused on testing the effectiveness of the source tracking method and analyzing key influences from an environmental aspect, such as the leakage rate curve, source location, flow field, and obstacles. For simplicity, we established a variety of source leakage scenarios in a two-dimensional ventilation room of dimension (X × Y = 12 m × 10 m) (Fig. 5). This room was ventilated with a supply air inlet (0.3 m) and an exhaust air outlet (0.4 m). Air was supplied at 0.8 m/s, and the air exchange rate was 7.2 air changes per hour, or 0.24 m^3/s.

We selected five locations (L1–L5) to analyze the effects of source location on the effectiveness of source tracking (Fig. 5a and Table 1). In each source tracking scenario, the hazardous gas CO (1.1233 kg/m^3) was released from one of the five locations, and the size of the leakage source was 0.1 m × 0.1 m. In some scenarios, we set four rectangular obstacles (O1–O4; Fig. 5b and Table 2) to test whether the method can be applied to environments with obstacles.

We assumed that the compressed gas was leaked isothermally from a rigid container with fixed volume. When the leakage begins, the gas pressure in the pipe is far greater than the ambient pressure, the leakage gas at the outlet is critical state, which is predominant in the total leakage process [47–49]. In some cases, this type of leakage is close to critical leakage more than 75% of the time during a complete leakage period [47]. Therefore, it can be treated as a critical leakage, and its leakage rate over time can be expressed as [47–50]:

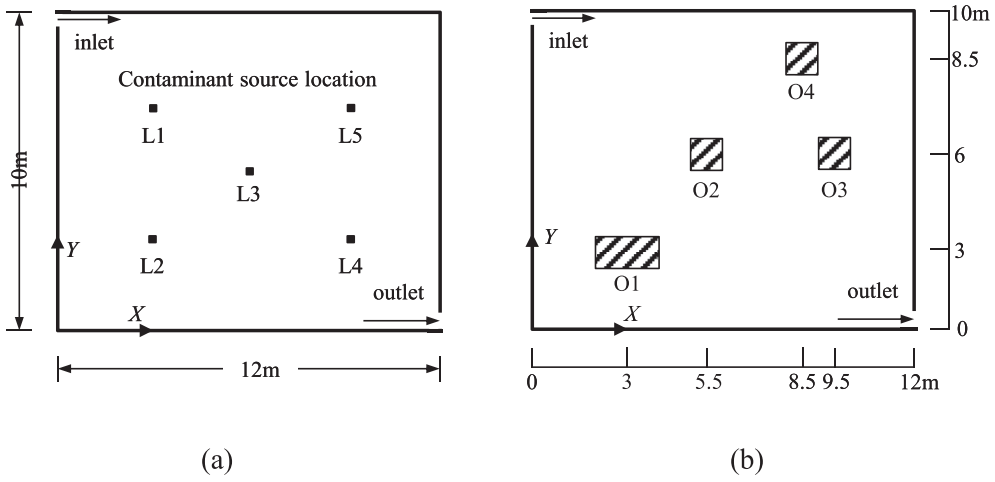

Fig. 5. Schematic of ventilation room: (a) potential source locations, (b) layout of obstacles.

Table 1
Potential source locations.

Source number	Coordinates of source center (m)	
	X	Y
L1	3.0	7.0
L2	3.0	3.0
L3	6.0	5.0
L4	9.0	3.0
L5	9.0	7.0

Table 2
Setup of obstacles.

Obstacle number	Start point (m)		End point (m)	
	X	Y	X	Y
O1	2.0	2.0	4.0	3.0
O2	5.0	5.0	6.0	6.0
O3	9.0	5.0	10.0	6.0
O4	8.0	8.0	9.0	9.0

$$Q(t) = Q_0(1 + k_1 t)^{k_2}, \tag{5}$$

where $Q(t)$ is the leakage rate at time t (mg/s); Q_0 is the initial leakage rate (mg/s); k_1 is the parameter depends on leakage characteristics and the surrounding environment (s^{-1}); k_2 is a constant depends on the ratio of specific heats of the gas at constant pressure and constant volume.

We established four leakage rate curves (S1–S4) to analyze effects of the time-varying leakage rate on the effectiveness of source tracking (Table 3 and Fig. 6). As shown in Fig. 6, S1 is the steepest decay curve, and represents scenarios with dramatic change of leakage rate. S4 is a horizontal curve, which represents scenarios with constant leakage rate. Curves S2 and S3 represent scenarios with moderate or slight change of leakage rate.

3.3. Setup of CFD simulations

FLUENT was used to simulate the indoor airflow field and gas dispersion. This software has been widely used and validated in indoor airflow and gas dispersion studies, as reported by Awadalla et al. [30].

Dispersion of the leakage source was simulated based on a steady indoor airflow field. A RNG $k-\varepsilon$ model, which has good accuracy for many flows, was used to simulate indoor turbulent flow [51,52]. An enhanced wall function was used to deal with airflow near the wall. A preprocessing program, Gambit, was used to generate the computational mesh. To reflect details of the airflow field and gas dispersion at locations adjacent to leakage source, inlet, and outlet, grids around those locations were deliberately refined. The finite volume method was used to discretize the Reynolds averaged Navier-Stokes equations and averaged energy and mass conservation equations. The difference scheme was a second-order upwind scheme. The momentum equations were solved on non-uniform staggered grids using a Semi-Implicit Method for Pressure-Linked Equations algorithm. Linear under-relaxation iteration was used to ensure convergence.

Table 3
Parameters of leakage rate curves.

Number of the curve	S_0 (mg/s)	k_1 ($10^{-4}\cdot s^{-1}$)	k_2
S1	1030.12	4.64	−7.67
S2	579.60	2.61	−7.67
S3	257.80	1.16	−7.67
S4	64.44	0.00	−7.67

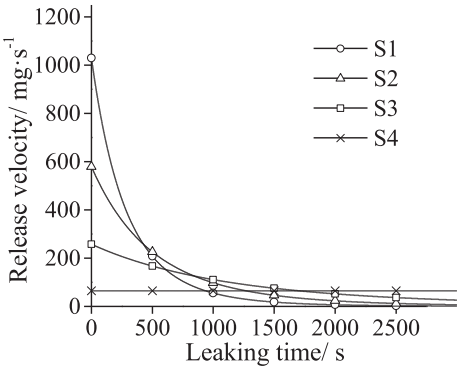

Fig. 6. Plot of leakage rate curves (S1–S4).

4. Results and discussion

4.1. CFD simulation results

To ensure grid-independent solutions, we conducted several grid independence tests. In an example test, we established six monitoring points (Fig. 7) and four mesh schemes (Table 4). As shown in Table 4, the results of Scheme 2 and Scheme 3 are close to those of Scheme 4. Scheme 3 was used for all the simulations would achieve higher accuracy than Scheme 2 and less computational load than Scheme 4. Therefore, we adopted Scheme 3 to reach a balance between accuracy and computational efficiency.

The steady-state indoor airflow field was simulated first, which showed a typical distribution of mixing ventilation (Fig. 8). Indoor air was driven by supply air injected from the inlet, and was finally exhausted by the outlet. A large vortex was created in the middle of the room, and two small vortexes were created in the lower-left and upper-right corners.

4.2. Effects of time-varying leakage rate

To validate the effectiveness of our method for tracking the sources with different leakage rate curves, four cases were established, (L1, S1), (L1, S2), (L1, S3), and (L1, S4). L1 represents the source location (Fig. 5, Table 1) and S1–S4 the leakage rate curves (Table 3, Fig. 6). In each case, five robots (R1–R5) began to localize

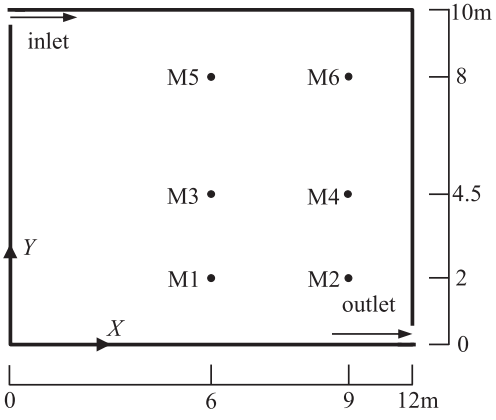

Fig. 7. Layout of monitoring points.

Table 4
Concentrations at monitoring points.[a]

Scheme	Number of grids	Mass fraction of CO(%)					
		M1(6 m, 2 m)	M2(9 m, 2 m)	M3(6 m,4.5 m)	M4(9 m,4.5 m)	M5(6 m,8 m)	M6(9 m,8 m)
1	3148	3.46	6.34	0.85	8.39	15.7	9.12
2	12384	4.54	7.14	0.78	9.44	16.1	9.33
3	45669	4.89	7.11	1.35	10.1	15.4	8.72
4	76611	5.19	7.45	1.59	10.6	15	8.67

[a] M1–M6 are the monitoring points (Fig. 7), and concentrations were sampled 120 s after leakage.

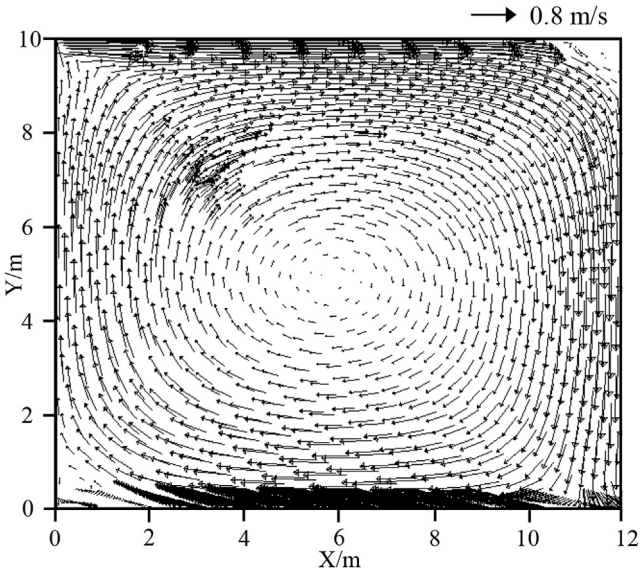

Fig. 8. Velocity field at time of source emission.

the leakage source at 120 s after leakage, from the same location (11.8 m, 0.2 m). The speed of each robot was 0.3 m/s.

The source tracking tests succeeded in all four cases. Taking case (L1, S1) as an example, which represents the scenarios with dramatic change of leakage rate, the source tracking procedure of the robots is shown in Fig. 9. After a leakage duration of 120 s, the robots were moving with the divergence search strategy. At the beginning, R4 was the first to find the plume, all robots except R4 converged to the location of R4 (Fig. 9a and b). After three seconds, a higher concentration of CO was detected by R1 in the convergence process, and then all robots except R1 turned their direction to R1 (Fig. 9c and d). Subsequently, the robots used the PSO algorithm to track the plume, successfully localizing the source 192 s after departure (Fig. 9e and f). Thus, from departure to successful source declaration, the overall localization time was 192 s, during which the leakage rate of the source declined to 35.5% of its original level.

The trajectories of robots R1–R5 in case (L1, S1) are shown in Fig. 10. First, the robots used a divergence search strategy to search as much area as possible. The robots diverged from the lower-right corner at their maximum speed. The trajectories are straight lines, which uniformly divided a horizontal plane into four identical angles. After the plume was first found by R4 (Fig. 10a), all robots were instructed to use the PSO algorithms to track the plume. The speed and direction of the robots were adjusted as shown by the square in Fig. 10b, and their trajectories were changed to meandering curves.

The circles in Fig. 10 refer to local extremum areas with high concentration levels. When a robot was trapped in one of these areas, it first repeated random movements and then used the divergence of mass flux method to determine whether that area was the actual source. If not, each robot initialized its fitness value and used the divergence search strategy again to exit the area. Otherwise, the robots reported the source location and terminated source tracking. As shown in Fig. 10, after exiting two local extremum areas, the robots finally succeeded in finding the actual leakage source.

The divergence search strategy and PSO algorithm are both random methods. Therefore, the trajectories of robots were also random in each tracking experiment. To reveal the effects of time-varying leakage rates on source tracking, we conducted 20 independent experiments for each of the four cases. All experiments had the same configuration, such as the initial location of robots, source tracking strategy, and maximum robot speed. Generally, the more gentle the leakage rate curve is, or the less change of leakage rate over time, the smaller the fluctuation of the results. Fig. 11 shows statistical results of the four cases. Except for case (L1, S3), quartile, average, maximum and minimum values of the overall source tracking time declined with decrease in the temporal change of leakage rate. Similar results were also obtained for source locations L2–L5. These results indicate that the source tracking may be more difficult for scenarios with more dramatic temporal change of leakage rate. In contrast, the source tracking may be easier for scenarios with smaller change of leakage rate or a constant rate. The exceptional result of case (L1, S3) may be attributed to an inadequate number of independent experiments.

4.3. Effects on location of leakage source

To test whether the method can successfully localize leakage sources in different locations, we established five cases, i.e., (L1, S2), (L2, S2), (L3, S2), (L4, S2) and (L5, S2). S2 represents release characteristics curve of the leakage source per Equation (5) and L1 through L5 represent the location of the leakage source in Fig. 12. In each case, five robots (R1–R5) began to localize the leakage source 120 s after leakage from the same location (11.8 m, 0.2 m). The robots successfully localized the source in all cases. The route of R3 in the five cases is shown in Fig. 12. The experimental results show that the method can effectively localize indoor leakage sources at different locations.

To further analyze the effects of leakage source location on the localization procedure, we designed 20 independent tests for each case. In each test, for the initial location of R1 to R5, the localization strategies and maximum speeds were the same. For leakage sources in the same location, the localization time is random because of randomness in the localization method. Fig. 13 shows statistical results. This figure shows that for leakage sources in different locations, the localization time varies greatly. The maximum localization time is 380 s and the minimum 37 s, and factor of 10 difference. These results show that the location of the leakage source has a strong effect on the time and difficulty of localization. Furthermore, it is seen in Fig. 13 that L5 is closest to the initial location of the robot, but the average localization time in case (L5, S2) is not the shortest. L1 is farthest from the initial robot location,

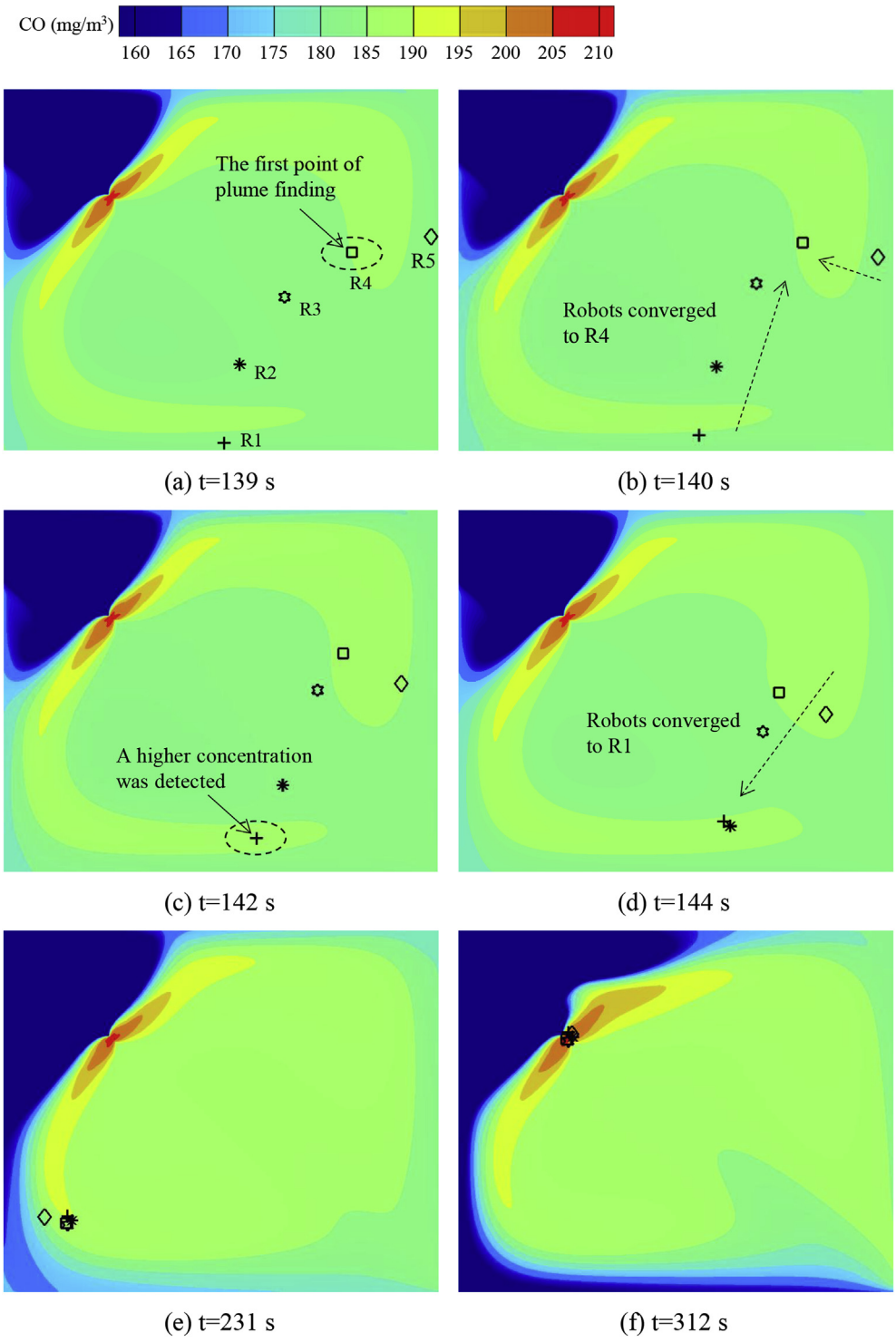

Fig. 9. Procedure of contaminant source localization in (L1, S1) case.

but the average localization time in case (L1, S2) is not the longest. These findings show that the required time for robot localization or localization difficulty does not completely depend on the distance between robot and leakage source.

4.4. Influences of barriers

To test whether the method is applicable to an environment with barriers, we added four rectangular barriers O1 through O4 (Fig. 5 and Table 2) based on case (L1, S2), with case number (L1, S2, O). In that case, the quantity of robots, initial location, time of departure, and maximum speed are the same as that in case (L1, S2). A barrier hinders robot motion and influences the distribution of gas concentration and flow field.

The trajectories of robots R1 and R4 in cases (L1, S2) and (L1, S2, O) are shown in Fig. 14. It is seen from the route within an

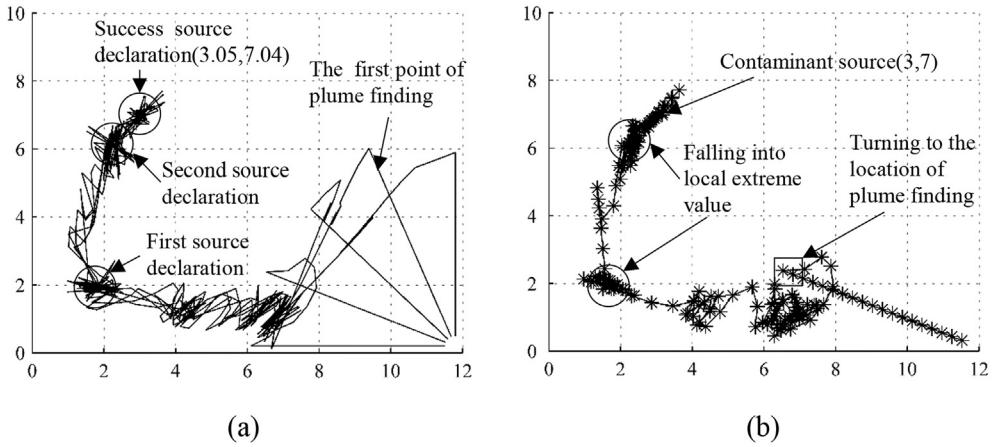

Fig. 10. Trajectories of robots in case (L1, S1): (a) trajectories of R1–R5, (b) trajectory of R2.

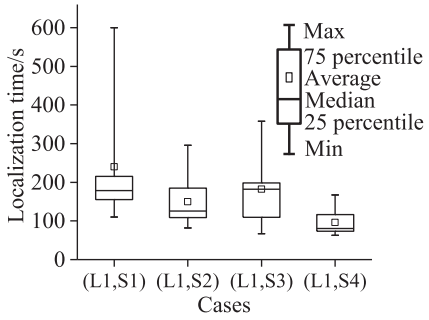

Fig. 11. The statistical results of overall source tracking time for four cases.

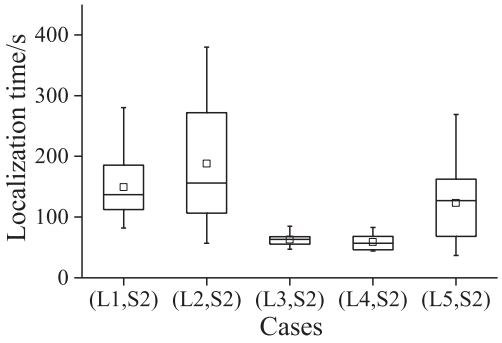

Fig. 13. Statistical analysis of experimental results for different leakage sources.

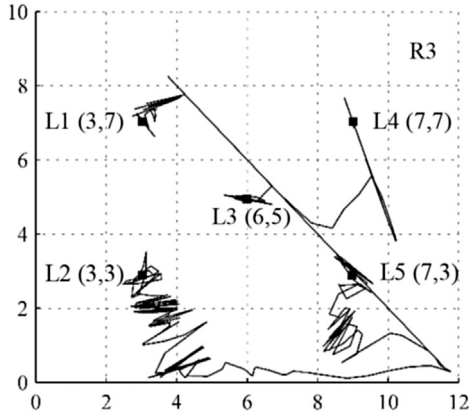

Fig. 12. Tracks of R3 in different cases.

imaginary circle shown in Fig. 14a and b that during the period of random search, the trajectory became more circuitous if robot R4 had to avoid barrier O3. After the plume was found, robot R1 avoided the barrier and got close to the leakage source at the same time.

To further analyze the influence of leakage source location on localization, we designed 20 independent tests for cases (L1, S2, O) and (L1, S2). Fig. 15 shows statistical results of localization time required for robots in the 20 tests in two cases. Unexpectedly, the robot localization time in case (L1, S2, O) was shorter than that in case (L1, S2). There are two main reasons for this. First, the diversion of the robot makes it easy to approach the leakage source if it wants to avoid the barrier. Second, the robot avoided a local extremum area during its avoidance of the barrier. Superficially, the barrier hinders robot movement, but for localization of the leakage source, the barrier is not necessarily disadvantageous; the result is case dependent.

5. Limitations of research

The proposed source localization method for an indoor time-varying leakage source is mainly composed of divergent search strategies, the PSO algorithm and mass flux divergence method. By adjusting robot movement, the method can solve a continuous leakage source localization problem with decaying emission characteristics in an indoor ventilation environment.

Learning from the experiences of other researchers [18,28], we used two-dimensional ventilation environments to validate the feasibility of the proposed method. This simplification can significantly reduce the computation loads of CFD simulations and the complexity of the source localization method. As a result, we can establish a variety of gas leak scenarios to reveal the influences on source localization of source intensity variation, source location, obstacles, flow field, and other factors. The results and conclusions of the present work cannot be directly extrapolated to actual three-dimensional cases, but the experience gained can provide a basis for extending the two-dimensional method to a three-dimensional one.

We assumed that the robot has no volume and its movement does not affect the flow field and gas concentration distribution. In practice, the scale of the robot is normally much smaller than that of the ventilation room, and the scale of the sensor is normally

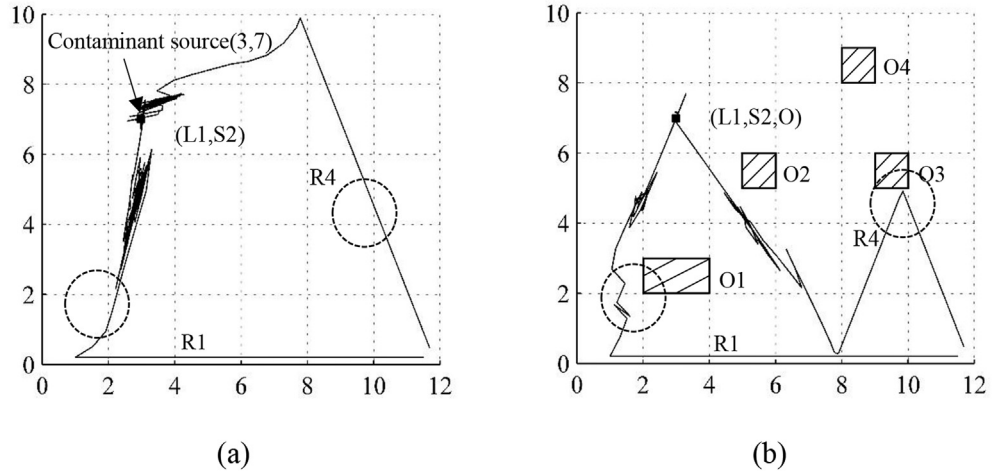

Fig. 14. Routes of robots R1 and R4: (a) trajectory in environment without barriers, (b) trajectory in environment with barriers.

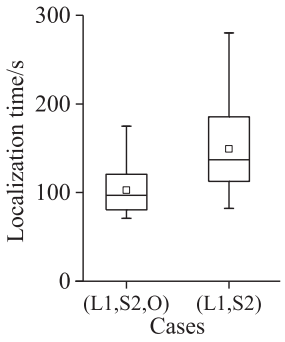

Fig. 15. Statistical results of leakage source localization time in cases (L1, S2, O) and (L1, S2).

much smaller than that of the robot. Moreover, to reduce the effects of robot movement on air velocity and gas concentration at the position of measuring point, we can separate sensors from main body of a robot by using a thin rod or string. For these reasons, this assumption is reasonable and was adopted in several studies [18,28,30]. In cases in which the scale of the space is small, and sensor is not large, or the sensor must inhale a certain amount of gas to analyze concentration, we should carefully evaluate whether this assumption is appropriate.

This study neglected the delay of sensor measurement. In an actual environment, the sensor detects gas with a time delay, but this does not affect concentration data using a correction. To help meet the needs of practical application, in future studies we will do correction in accordance with delay characteristics of the sensor.

6. Conclusions

In this work, a robot with sensor system was used to find the location of a leakage source, thereby providing a solution to a time-varying leakage source problem. The source localization method for such a source was divided into three phases: divergent search strategy discovery of the plume, PSO algorithm to track the plume, and mass flux divergence method to confirm the location of the leakage source. Based on our time-varying leakage source localization method, the robots were used to verify method effectiveness through indoor two-dimensional ventilation room simulation experiments. We analyzed the influences of intensity change, location, and obstacles on the localization procedure.

Based on the time-varying leakage source localization method, the following conclusions were drawn through case study.

1. The method can solve the problem of time-varying source localization under different ventilation environments, intensity variations, and obstacles.
2. Change of intensity of the time-varying source increases the time of localization. The smaller the rate of change, the shorter the time of leakage source localization. Statistical experiments show that the smaller the change rate of release intensity of the leakage source, the narrower the fluctuation range of test results, and the fewer the difficulties in locating the leakage source.
3. In the location of the various leakage sources, the time of robot localization varies substantially. This time or difficulty does not entirely depend on the distance between robots initial location and the leakage source.
4. The presence of an obstruction does not necessarily increase the time of leakage source localization. Although it is apparent that such obstructions can impede robot movement and may alter the distribution of indoor flow fields and contaminants, whether the obstacle is favorable or unfavorable to robot localization is case-dependent.

Based on the localization of time-varying leakage sources, detection values of robot sensors can theoretically solve the problem of source strength identification. We have researched source strength identification. This paper highlights the influence of ventilation forms and obstacles and other environmental factors on source localization. In further studies, we will analyze the influence of these factors on source localization from the aspects of mobile robot number, motion speed, sensor thresholds and response time, thereby optimizing the time-varying source localization method. In such studies, we will verify the method in an actual ventilation environment using tracer gas experiments in tandem with mobile robots.

Acknowledgements

This study was supported by the National Natural Science Foundation of China (Grant No. 51478468) and the National Program on Key Basic Research Project (973 Program, Grant No. 2015CB058000).

Appendix A. Collision avoidance algorithm

In practice, each robot can be equipped with five ultrasonic sensors to detect an obstacle in front of the robot. As shown in Fig. A1, these sensors can detect obstacles in five directions. Detected distances between the robot and obstacle in the left, middle-left, front, middle-right, and right directions are denoted d_l, d_{ml}, d_f, d_{mr} and d_r, respectively.

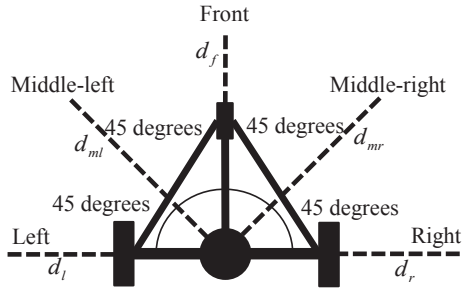

Fig. A.1. Ultrasonic sensors setting for measuring five directions.

For a moving robot, when the distance detected by any one of the five ultrasonic sensors drops below threshold d_T, a collision avoidance algorithm is triggered to adjust the robot movement. As illustrated in Fig. A2, the robot will maintain the same speed of movement but change its direction to avoid an obstacle. The logic diagram of the collision avoidance algorithm is shown in Fig. A3. The deflection angle 2θ of robot velocity can be calculated by a cosine function. Both intersection angles at times t and $t + \Delta t$ between the robot velocity and obstacle plane are of the same magnitude.

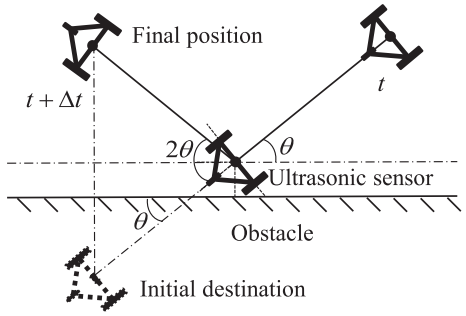

Fig. A.2. Schematic of mobile robot for obstacle avoidance.

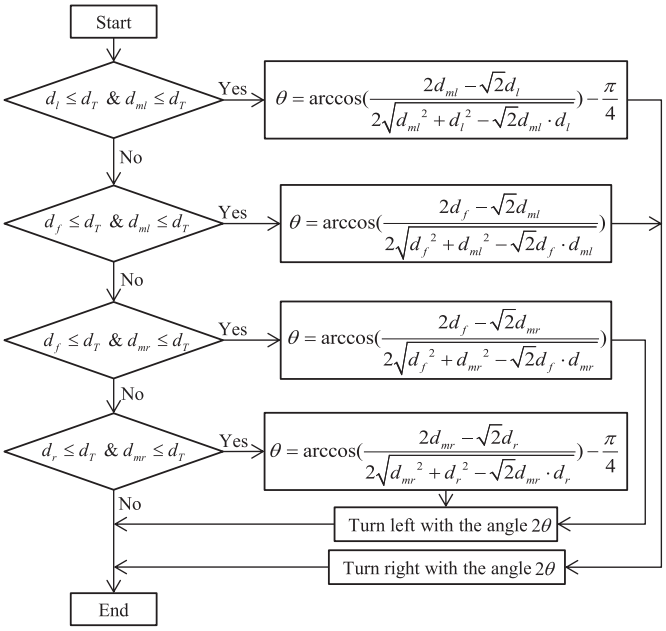

Fig. A.3. Logic diagram of collision avoidance algorithm.

References

[1] A.R. Anderson, Health effects of cut gas lines and other petroleum product release incidents-seven states, 2010–2012, MMWR Morb. Mortal. Wkly. Rep. 64 (22) (2015) 601–605.

[2] T.F. Zhang, H.Z. Li, S.G. Wang, Inversely tracking indoor airborne particles to locate their release sources, Atmos. Environ. 55 (3) (2012) 328–338.

[3] H. Cai, X.T. Li, Z.L. Chen, L.J. Kong, Fast identification of multiple indoor constant contaminant sources by ideal sensors: a theoretical model and numerical validation, Indoor Built Environ. 22 (6) (2013) 897–909.

[4] T. Zhang, S. Yin, S. Wang, An inverse method based on CFD to quantify the temporal release rate of a continuously released pollutant source, Atmos. Environ. 77 (3) (2013) 62–77.

[5] P. Kathirgamanathan, R. McKibbin, R.I. McLachlan, Source release-rate estimation of atmospheric pollution from a non-steady point source at a known location, Environ. Model Assess. 9 (1) (2004) 33–42.

[6] P. Sreedharan, M.D. Sohn, W.W. Nazaroff, A.J. Gadgil, Influence of indoor transport and mixing time scales on the performance of sensor systems for characterizing contaminant releases, Atmos. Environ. 41 (40) (2007) 9530–9542.

[7] M.D. Sohn, P. Reynolds, N. Singh, A.J. Gadgil, Rapidly locating and characterizing pollutant releases in buildings, J. Air Waste Manage 52 (12) (2002) 1422–1432.

[8] V. Vukovic, P.C. Tabares-Velasco, J. Srebric, Real-time identification of indoor pollutant source positions based on neural network locator of contaminant sources and optimized sensor networks, J. Air Waste Manage 60 (9) (2010) 1034–1048.

[9] A. Bastani, F. Haghighat, J.A. Kozinski, Contaminant source identification within a building: toward design of immune buildings, Build. Environ. 51 (5) (2012) 320–329.

[10] H. Cai, X. Li, Z. Chen, M. Wang, A fast model for identifying multiple indoor contaminant sources by considering sensor threshold and measurement error, Build. Serv. Eng. Res. T 36 (1) (2014) 89–106.

[11] H. Cai, X. Li, Z. Chen, M. Wang, Rapid identification of multiple constantly-released contaminant sources in indoor environments with unknown release time, Build. Environ. 81 (7) (2014) 7–19.

[12] D. Liu, F.Y. Zhao, H.Q. Wang, E. Rank, History source identification of airborne pollutant dispersions in a slot ventilated building enclosure, Int. J. Therm. Sci. 64 (64) (2013) 81–92.

[13] T. Zhang, Q. Chen, Identification of contaminant sources in enclosed spaces by a single sensor, Indoor Air 17 (6) (2007) 439–449.

[14] Z.Q. Zhai, X. Liu, H.D. Wang, Y.G. Li, J.J. Liu, Experimental verification of tracking algorithm for dynamically-releasing single indoor contaminant, Build. Simul. 5 (1) (2012) 5–14.

[15] T. Zhang, H. Zhou, S. Wang, Inverse identification of the release location, temporal rates, and sensor alarming time of an airborne pollutant source, Indoor Air 25 (4) (2015) 415–427.

[16] L.L. Wang, X.Y. You, Identification of indoor contaminant source location by a single concentration sensor, Air Qual. Atmos. Hlth 8 (1) (2015) 115–122.

[17] P. Pyk, S.B.I. Badia, U. Bernardet, P. Knusel, M. Carlsson, J. Gu, E. Chanie, B.S. Hansson, T.C. Pearce, P. Verschure, An artificial moth: chemical source

localization using a robot based neuronal model of moth optomotor anemotactic search, Auton. Robot. 20 (3) (2006) 197–213.
[18] J.G. Li, Q.H. Meng, Y. Wang, M. Zeng, Odor source localization using a mobile robot in outdoor airflow environments with a particle filter algorithm, Auton. Robot. 30 (3) (2011) 281–292.
[19] N. Voges, A. Chaffiol, P. Lucas, D. Martinez, Reactive searching and infotaxis in odor source localization, PLoS Comput. Biol. 10 (10) (2014) e1003861.
[20] R.A. Russell, A. Bab-Hadiashar, R.L. Shepherd, G.G. Wallace, A comparison of reactive robot chemotaxis algorithms, Robot. Auton. Syst. 45 (2) (2003) 83–97.
[21] D.J. Harvey, T.F. Lu, M.A. Keller, Comparing insect-inspired chemical plume tracking algorithms using a mobile robot, IEEE T. Robot. 24 (2) (2008) 307–317.
[22] A. Marjovi, L. Marques, Multi-robot olfactory search in structured environments, Robot. Auton. Syst. 59 (11) (2011) 867–881.
[23] Q.H. Meng, W.X. Yang, Y. Wang, F. Li, M. Zeng, Adapting an ant colony metaphor for multi-robot chemical plume tracing, Sensors 12 (4) (2012) 4737–4763.
[24] A.T. Hayes, A. Martinoli, R.M. Goodman, Swarm robotic odor localization: off-line optimization and validation with real robots, Robotica 21 (4) (2003) 427–441.
[25] L. Marques, U. Nunes, A. de Almeida, Olfaction-based mobile robot navigation, Thin Solid Films 418 (1) (2002) 51–58.
[26] H. Ishida, H. Tanaka, H. Taniguchi, T. Moriizumi, Mobile robot navigation using vision and olfaction to search for a gas/odor source, Auton. Robot. 20 (3) (2006) 231–238.
[27] A. Lilienthal, T. Duckett, Building gas concentration gridmaps with a mobile robot, Robot. Auton. Syst. 48 (1) (2004) 3–16.
[28] Z.Z. Liu, Y.J. Wang, T.F. Lu, Odor source localization using multiple robots in complicated city-like environments, Adv. Mat. Res. 291–294 (2011) 3337–3344.
[29] A. Marjovi, L. Marques, Optimal spatial formation of swarm robotic gas sensors in odor plume finding, Auton. Robot. 35 (2) (2013) 93–109.
[30] M. Awadalla, T.F. Lu, Z.F. Tian, B. Dally, Z. Liu, 3D framework combining CFD and MATLAB techniques for plume source localization research, Build. Environ. 70 (12) (2013) 10–19.
[31] G. Kowadlo, R.A. Russell, Robot odor localization: a taxonomy and survey, Int. J. Robot. Res. 27 (8) (2008) 869–894.
[32] A.J. Lilienthal, A. Loutfi, T. Duckett, Airborne chemical sensing with mobile robots, Sensors 6 (11) (2006) 1616–1678.
[33] A.T. Hayes, A. Martinoli, R.M. Goodman, Distributed odor source localization, IEEE Sens. J. 2 (3) (2002) 260–271.
[34] W. Li, J.A. Farrell, S. Pang, R.M. Arrieta, Moth-inspired chemical plume tracing on an autonomous underwater vehicle, IEEE T. Robot. 22 (2) (2006) 292–307.
[35] Z. Pasternak, F. Bartumeus, F.W. Grasso, Lévy-taxis: a novel search strategy for finding odor plumes in turbulent flow-dominated environments, J. Phys. A Math. Theor. 42 (43) (2009) 434010.
[36] P.P. Neumann, V.H. Bennetts, A.J. Lilienthal, M. Bartholmai, J.H. Schiller, Gas source localization with a micro-drone using bio-inspired and particle filter-based algorithms, Adv. Robot. 27 (9) (2013) 725–738.
[37] T. Lochmatter, A. Martinoli, Tracking odor plumes in a laminar wind field with bio-inspired algorithms, in: O. Khatib, V. Kumar, G.J. Pappas (Eds.), Experimental Robotics, Springer, Berlin, 2009, pp. 473–482.
[38] M. Vergassola, E. Villermaux, B.I. Shraiman, 'Infotaxis' as a strategy for searching without gradients, Nature 445 (7126) (2007) 406–409.
[39] Y. Tian, X.D. Kang, Y.Y. Li, W. Li, A.Q. Zhang, J.C. Yu, Y.P. Li, Identifying rhodamine dye plume sources in near-shore oceanic environments by integration of chemical and visual sensors, Sensors 13 (3) (2013) 3776–3798.
[40] D.V. Zarzhitsky, D.F. Spears, D.R. Thayer, Experimental studies of swarm robotic chemical plume tracing using computational fluid dynamics simulations, Int. J. Intell. Comput. Cybern. 3 (4) (2010) 631–671.
[41] W. Jatmiko, K. Sekiyama, T. Fukuda, A pso-based mobile robot for odor source localization in dynamic advection-diffusion with obstacles environment: theory, simulation and measurement, IEEE Comput. Intell. M. 2 (2) (2007) 37–51.
[42] M. Tavakoli, G. Cabrita, R. Faria, L. Marques, A. de Almeida, Cooperative multi-agent mapping of three-dimensional structures for pipeline inspection applications, Int. J. Robot. Res. 31 (12) (2012) 1489–1503.
[43] H. Ishida, Y. Wada, H. Matsukura, Chemical sensing in robotic applications: a review, IEEE Sens. J. 12 (11) (2012) 3163–3173.
[44] W. Li, Identifying an odour source in fluid-advected environments, algorithms abstracted from moth-inspired plume tracing strategies, Appl. Bionics Biomech. 7 (1) (2010) 3–17.
[45] L. Marques, U. Nunes, A. de Almeida, Particle swarm-based olfactory guided search, Auton. Robot. 20 (3) (2006) 277–287.
[46] S.L. Sabat, S.K. Udgata, K.P.N. Murthy, Small signal parameter extraction of MESFET using quantum particle swarm optimization, Microelectron. Reliab 50 (2) (2010) 199–206.
[47] Z.L. Liu, H.F. Wang, Y.X. Li, Environmental heating effects on the gas parameters during the long-distance gas pipelines leakage process, Front. Environ. Sci. Eng. China 4 (1) (2015) 11–19.
[48] N. Bariha, I.M. Mishra, V.C. Srivastava, Hazard analysis of failure of natural gas and petroleum gas pipelines, J. Loss Prev. Proc. 40 (2016) 217–226.
[49] Y.D. Jo, B.J. Ahn, A simple model for the release rate of hazardous gas from a hole on high-pressure pipelines, J. Hazard. Mater 97 (1–3) (2003) 31–46.
[50] H. Montiel, J. Vilchez, J. Casal, J. Arnaldos, Mathematical modelling of accidental gas releases, J. Hazard. Mater 59 (2–3) (1998) 211–233.
[51] Z. Han, R.D. Reitz, Turbulence modeling of internal combustion engines using RNG κ-ε models, Combust. Sci. Technol. 106 (4–6) (1995) 267–295.
[52] J.D. Posner, C.R. Buchanan, D. Dunn-Rankin, Measurement and prediction of indoor air flow in a model room, Energ. Build. 35 (5) (2003) 515–526.